Materials Advances

ROYAL SOCIETY OF CHEMISTRY

PAPER

View Article Online
View Journal | View Issue

Check for updates

Cite this: *Mater. Adv.*, 2026, 7, 3681

Effect of halloysite nanotube addition on mechanical and thermal performance of banana/cotton hybrid natural fiber-reinforced polymer nanocomposites

G. Umachitra,[a] P. S. Sampath,[b] A. Karthik,[c] M. S. Senthilkumar,[d] K. Ramachandran,[e] L. Rajeshkumar*[f] and M. Sathishkumar*[g]

Received 16th December 2025,
Accepted 19th February 2026

DOI: 10.1039/d5ma01471a

rsc.li/materials-advances

Natural fibre composite materials can replace conventional and synthetic materials in real-world applications where energy and weight conservation are necessary. This research investigates the effects of halloysite nanotubes (HNTs) and alkali treatment on banana/cotton hybrid woven fabric reinforced with epoxy composites. The mechanical and thermal properties and morphological aspects of cotton/banana fabric-reinforced epoxy composites-filled with HNTs and also the unfilled composites were evaluated. The cotton/banana hybrid epoxy composites were enhanced with halloysite nanotubes in 1, 2, 3, and 5 wt%. The chemical structure, and surface morphology of composite materials were analysed by using SEM and FTIR. The mechanical properties such as tensile, flexural, compression, and impact strengths were assessed according to ASTM standards. The results demonstrate that composites with 2 wt% HNTs possess optimal tensile (62 MPa) and flexural strength (102 MPa), whereas greater filler loadings caused agglomeration, and decreasing characteristics. Furthermore, thermal studies revealed that the composites with 2 wt% HNTs exhibited higher thermal stability, with degradation occurring between 357 °C and 452 °C. Morphology portrayed that the superior bonding and surface homogeneity in the 2 wt% HNT nanocomposite. This study highlights the importance of nanofillers and surface treatment in addressing the constraints of natural fibre composites, permitting their application across several industries, including automotive, aerospace, and construction.

1. Introduction

Composite materials represent a handy category of resources with diverse applications and superior properties. Synthetic fibres are commonly used in polymer composites as reinforcement, but the incorporation of renewable resources to address environmental concerns is a growing trend. Natural fibres, with their technological advantages and ecological benefits, can be used as biodegradable reinforcing agents, and thus, they are a perfect substitute for synthetic fibres in the composite industry.[1,2] The mechanical properties and chemical makeup of several natural fibres have been well described, emphasising their potential in an extensive collection of applications, including the automotive, structural, architectural, and aerospace industries.[3–5] Numerous factors contribute to the increasing preference for natural fibre reinforced polymer composites (NFRPCs). These include their cost-effectiveness, lightweight nature, reduced carbon dioxide emissions, non-abrasiveness, minimal skin irritation, and limited health risks. NFRPCs not only enhance durability but they also offer significant environmental benefits, reinforcing their status as a sustainable choice in composite materials.[6–9]

While natural fibres offer numerous advantages, they also present certain drawbacks. These include issues such as unsuitability among fibres and matrix, poor moisture resistance, dimensional variability, and a tendency to clump during handling.[10] Subpar interfacial bonding between hydrophilic

---

[a] Department of Textile Technology (Design and Weaving), SSM Polytechnic College, Komarapalayam 638183, Tamil Nadu, India
[b] Department of Mechanical Engineering, K.S. Rangasamy College of Technology, Tiruchengode 637215, Tamil Nadu, India
[c] Department of Mechatronics Engineering, Akshaya College of Engineering and Technology, Coimbatore 642109, Tamil Nadu, India
[d] Department of Mechanical Engineering, Excel Engineering College, Komarapalayam 637303, Tamil Nadu, India
[e] Department of Chemistry, Kangeyam Institute of Technology, Kangeyam, Tiruppur, 638108, Tamil Nadu, India
[f] CoE-Advanced Materials Synthesis and Department of Mechanical Engineering, Alliance School of Applied Engineering, Alliance University, Bangalore 562106, Karnataka, India. E-mail: lrkln27@gmail.com
[g] Department of Mechanical Engineering, Amrita School of Engineering, Amrita Vishwa Vidyapeetham, Chennai 601103, India. E-mail: m_sathishkumar@ch.amrita.edu

natural fibres and hydrophobic polymer matrices negatively affects the properties of the composite, posing challenges for manufacturing and structural uses.[11] However, these problems can be solved by changing the chemicals in the reinforcing fibres, mixing different materials, or adding fillers.[12,13] The most common and fundamental technique to improve the bonding properties between natural fibres and the polymer matrix is alkali treatment, also known as mercerisation. This approach uses NaOH (sodium hydroxide) to modify the cellulose construction of natural fibers, facilitating the breakdown and separation of fiber strands. The alkali treatment effectively removes unwanted substances such as lignin, wax, and oil, resulting in a clean and unvarying surface that improves the overall efficiency of the composite.[11,14–18]

Hybridisation serves as an active strategy for augmenting the mechanical properties of composite materials. Hybridisation of various types of fibres can occur, concomitant with the integration of different nanofillers (NFs) or nanomaterials within a single matrix. This process results in hybrid nanocomposite materials that exhibit unique properties due to the synergistic effects of their combined components.[19–21] Because hybrid nanocomposites typically demonstrate improved strength, stiffness, and thermal constancy, they are appropriate for a wide array of applications in the automotive, aerospace, and construction industries, among others.[22–24]

Adding NFs using advanced manufacturing techniques has resulted in an improved interface between the fibre and matrix in fiber-reinforced composite materials.[25–27] These NFs can considerably boost the mechanical properties of composites, thereby broadening the choices that are available for potential applications. Effective mixing of NFs within the matrix leads to improved mechanical, thermal, and tribological properties due to their homogeneous dispersion.[28–30] Common inorganic NFs include materials such as alumina, titanium dioxide, magnesia, calcium carbonate silica, and zinc oxide. Naturally occurring organic NFs encompass synthetic clays, carbon black, and cellulose fibres.[31–34] While NFs are primarily inorganic, they can also comprise organic substances, reflecting the diverse options available for enhancing composite materials. The optimal quantity of NFs to use depends on a variety of factors, including the type of filler, fiber, and matrix used.[35–40]

Halloysite nanotubes (HNTs) are aluminosilicate nanotubes with the chemical formula $Al_2Si_2O_5(OH)_4{\cdot}2H_2O$, and these nanotubes are inexpensive when compared with other nanotubes such as carbon nanotubes. The homogenous dispersion of HNTs in polymer composites enhances the mechanical and thermal properties of the composite, but their inherent disadvantage is their agglomeration.[41–43] HNTs possess a tubular structure, with the size of the particles ranging from 0.2 to 2 microns, while the inner and outer diameters range from 10–40 to 40–70 nm, respectively. These dimensions of the HNTs facilitate increased load transfer to the polymer matrix, and hence, enhancement of the mechanical properties of polymer matrix composites is possible.[44–46]

It was stated in a few research works that HNTs facilitate the bond formation between the polymer matrix and the reinforcements, which requires additional mechanical force to break, thereby enhancing the mechanical properties of the HNT-based polymer composites.[47–50] Experiments have been performed that used carbon nanotubes (CNTs), HNTs, and graphene oxide (GO) as reinforcements in glass fiber-based polyester composites. The mechanical properties of the composites were more optimal with 2 wt% HNTs, while a sharp decline in mechanical properties was witnessed beyond this proportion because of the agglomeration of the HNTs.[51] When HNTs were reinforced with natural fiber composites and when the proportions were maintained within 4 wt%, the mechanical, thermal, and viscoelastic properties of the composites were significantly enhanced. Beyond 4 wt%, various research works have reported agglomeration of the HNTs in the polymer matrix.[52,53]

Despite the ongoing interest in natural fibre composites, there remains a significant gap in the research regarding their enhancement, particularly in NFRPCs. The current study focusses on fabricating polymer composites reinforced with HNTs and hybridized with alkali-treated banana/cotton woven fabric. The composites were produced using a compression moulding process. The influences of surface treatment of the fibers and addition of HNTs to natural fiber hybrid composites were evaluated through mechanical tests such as tensile, flexural, and impact tests. To further understand the material behaviour, morphological properties were evaluated using scanning electron microscopy (SEM). The composites were also characterized through thermogravimetric analysis (TGA) and Fourier transform infrared (FTIR) spectroscopy.

2. Materials and methods

2.1. Materials

Banana/cotton plain woven fabric, with a weight of 164 g m^{-2} and a density of 1.48 g cm^{-3}, was purchased from Ganesh Traders in Kanuvakarai, Coimbatore, Tamil Nadu. Epoxy (LY 556), with a density range of 1.5–1.2 g cm^{-3}, and epoxy hardener HY951, with a density of 0.98 g cm^{-3}, were procured from Covai Seenu & Co. in Coimbatore, Tamil Nadu, India. The halloysite nanotubes were obtained from Otto Chemine Pvt. Ltd. in Mumbai, Maharashtra, India. The density of these tubes is 2.53 g cm^{-3}. The chemical composition of HNTs is alumina-silicate, as indicated in Table 1, and was determined using X-ray fluorescence.

2.2. Preparation of nanocomposites

The banana/cotton fabric was initially treated with 5% NaOH to increase its wettability with the epoxy matrix. The fabric was cut

Table 1 Constituents of HNTs

Constituents	Weight percentage (%)
SiO_2	50.4
Al_2O_3	35.5
Fe_2O_3	0.25
TiO_2	0.05

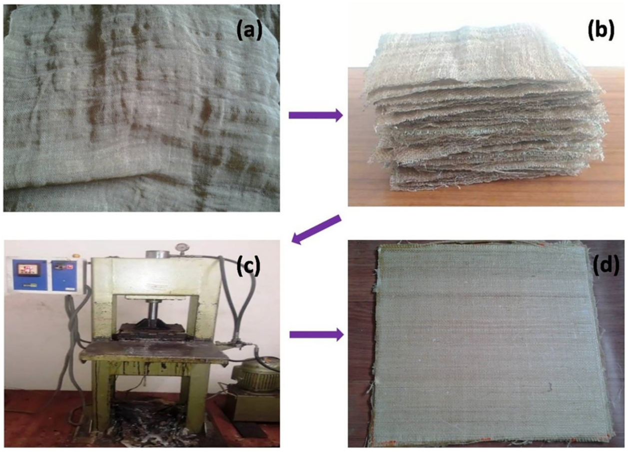

Fig. 1 Preparation of composite: (a) banana/cotton plain woven fabric, (b) required size of the woven fabric, (c) compression molding machine, and (d) nanocomposite material.

according to mould dimensions, and then soaked in NaOH solution for 2 hours. Then, the fibers were sun-dried for 16 hours, and hot air oven-dried for 2 hours at 60 °C. A rectangular mould composed of steel plates sized 270 × 270 × 3 mm was used in a compression moulding machine, which is shown in Fig. 1c. The HNTs were initially mixed with epoxy resin as per the chosen weight ratio, and were then mixed using an ultrasonic stirrer at a frequency of 20 Hz for 30 minutes for uniform dispersion of the HNTs in the epoxy matrix. The HNT epoxy resin was initially coated on each fabric layer, and the laminates were then placed in the mould, after which the mould was filled with the remaining quantity of the resin as per the proportion. Eight layers of the banana/cotton fabric were alternatively placed, which were subsequently placed inside the mould of the compression moulding machine. The machine carried out the moulding process for 3 hours, maintaining a pressure of 30 MPa and a temperature of 130 °C. To facilitate the removal of composite materials from the mould, a layer of wax was placed on the mould during the composite material fabrication process. Post-curing of the composites was carried out at 70 °C for 1 hour in an electric oven, and the final thickness of the composite plates varied from 3.6 to 4.1 mm. Five different combinations of nanocomposites were produced, as illustrated in Table 2.

Table 2 Composition of the nanocomposites

	Composition		
Specimen	Epoxy (wt%)	HNTs (wt%)	Banana/cotton fabric (wt%)
C_1	55	0	45
C_2	54	1	45
C_3	53	2	45
C_4	52	3	45
C_5	50	5	45

2.3. Mechanical testing

The manufactured nanocomposite materials were cut according to the standards of ASTM D3039 for tensile testing, ASTM D790 for flexural testing, ASTM D256 for impact testing, and ASTM D3410 for compression testing. The tensile, flexural, and compression tests were performed *via* a computerized universal testing machine (UTM) in line with ASTM recommendations. Five specimens were taken from each laminate for a specific experiment, and the average test result of these five samples was recorded as the final result. The impact test was conducted using an Izod impact test apparatus.

3. Results and discussion

3.1. Tensile strength of the composites

Fig. 2a illustrates the correlation between nanoparticles and tensile strength across various composite compositions.

The 0 wt% HNTs resulted in the lowest measurement, which was 51 MPa. From the C1 to C3 composites (0 wt% to 2 wt% HNTs), the values increased. The tensile strength increased to 62 MPa when the HNT loading reached 2 wt%. Shutava *et al.* observed the same trend in their study of HNT-loaded nanocomposites.[54] They discovered that when polymer nanocomposites with 5% HNTs were doped, the tensile strength increased by 30 to 50%. Further, the same result was found in various studies when adding nanofillers to polymers at a concentration of less than 5%, which improved the tensile characteristics of the polymers.[55–57] As the quantity of HNTs increased, the tensile strength diminished due to agglomeration, hence further reducing the tensile properties. This is the result of insufficient diffusion within the matrix. According to Yasmin *et al.*, increasing the amount of HNT particles negatively affected the modulus. This occurred because the production of exfoliated aggregates decreased the strength.[58]

3.2. Flexural strength of the composites

The three-point flexural test, commonly employed in this study, was used to assess the bending strength of composite materials. The evaluation procedure entailed placing the specimen in a UTM and spreading the force over it until it fractured. Fig. 2b provides a graphical representation of the collected results from the flexural testing. The flexural property of the nanocomposites is extreme at a nanotube loading of 2 wt%, with a value of 102 MPa. The curve exhibits a pattern similar to that of the tensile property. At a concentration of 0 wt% HNTs, the minimum value reached 68 MPa. As a result, the parabolic curve decreased with higher nanofiller loadings. When filler loading increased, the degree of contact between the matrix and fillers weakened, resulting in a decrease in mechanical properties.[59]

3.3. Compression strength of the nanocomposites

Fig. 2c displays the compression properties of the nanofiller loadings in various proportions. The graphical analysis indicates that the values for the tensile and flexural properties are likely to be nearly comparable, with minimal deviations.

The curve exhibited a very uniform trajectory with no increase in the characteristics until the addition of 2 wt% HNTs. The variation in values is not significant in terms of compression characteristics. This indicates that the effect of HNTs on the compressive features of the nanocomposites is very low. The extreme value of 72 MPa was attained with a 2 wt% concentration of HNTs, while the minimum value was obtained with no filler loading.

3.4. Impact strength of the nanocomposites

Fig. 2d illustrates the impact property values of the composites. The impact characteristic of the composites exhibits a similar pattern. At a concentration of 2 wt%, the nanoloading yields the maximum value, while a concentration of 4 wt% yields the minimum value. This demonstrates that the inclusion of microparticles enhances the impact property. Once the optimal value was reached, the impact property continued to be unaffected by the accumulation of additional nanoparticles. This is because the presence of a greater fraction of agglomerated particles hindered the efficient transmission of impact energy. Using nano-filled composites increased the impact property of unfilled polymer composites by approximately 44%.

The strengthening processes generated by the nanomaterials are responsible for the enhanced impact strength of the HNT-filled nanocomposites. The filler materials in composites limit the flexibility of the polymer sequence. This restriction hinders the capacity of composites to freely deform, thereby reducing their ductility. As a result, the HNT particles serve as shock absorbers during impact testing. There was a similar pattern in previous research on glass fibre-reinforced epoxy composites. The nanocomposites were infused with 1–5 wt% HNT particles. In this study, the concentration of nanoparticles was increased to 3 wt% before reducing it to 5 wt%. This work bears similarities to the current study, as it achieves the highest point at a concentration of 2 wt%, followed by a decline in the curve. This is due to the uneven spread of HNT particles in polymers, which causes cracks to spread in the material, and leads to the early breakdown of composites and results in subpar impact capabilities.[60,61]

3.5. Thermal analysis

The results shown in Fig. 1 reveal that the banana/cotton fabric reinforced with 1%, 2%, 3%, and 4% HNTs in each epoxy nanocomposite composition is much more stable at high temperatures as compared to regular composites. Heat causes moisture to evaporate in the specimen, initiating the degradation of hemicellulose and cellulose. Moreover, each laminate exhibited a weight reduction of 10 to 15% between 338 and 360 °C. The fundamental constituents of cellulose, hemicelluloses, and lignin are responsible for the significant weight reduction of 60 to 70% that typically occurs between 360 and 499 °C. In each specimen, between 585 and 595 °C, total decomposition of all combustible components and the generation of inorganic waste occurred. Table 3 demonstrates that the hybrid composite containing 2% HNTs exhibited the lowest residual weight at 600 °C (7.83%) in comparison to the other composites. This indicates that, relative to other hybrid polymer composites, superior experimental heat stability existed for cotton fibre.[38,58]

Fig. 3 displays the main thermograms for various fibre epoxy resin mixtures. These include the banana/cotton fabric reinforced with 1%, 2%, 3%, and 5% HNT composites. Thermogravimetric analysis was employed to evaluate the thermal degradation and stability of these composites at varying proportions. The stability temperature range was recorded between 30 °C to 600 °C. A 3.5% weight reduction indicated the onset of

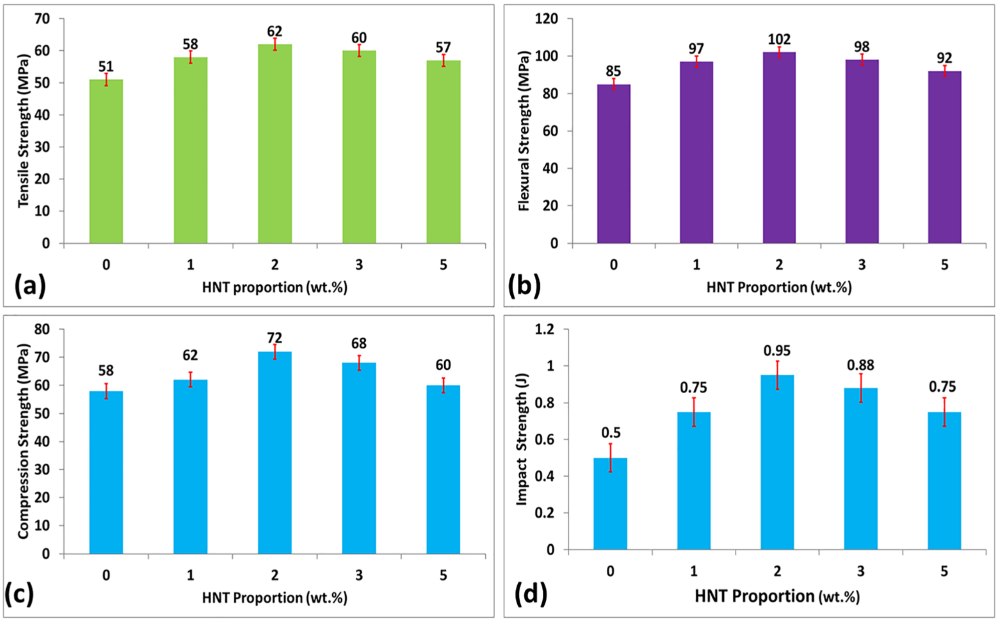

Fig. 2 Mechanical properties of HNT nanocomposites: (a) tensile strength, (b) flexural strength, (c) compressive strength, and (d) impact strength.

Table 3 TGA values for the hybrid nanocomposites

Thermal parameter	0 wt% HNTs	1 wt% HNTs	2 wt% HNTs	3 wt% HNTs	5 wt% HNTs
Initial degradation temperature °C	338.08	342.32	357.32	348.64	338.76
Final degradation temperature °C	420.84	429.03	452.64	432.38	427.52
Inflection point °C	388.63	395.47	416.38	392.13	383.38
Residue (%)	20.36	19.53	17.83	18.43	19.05

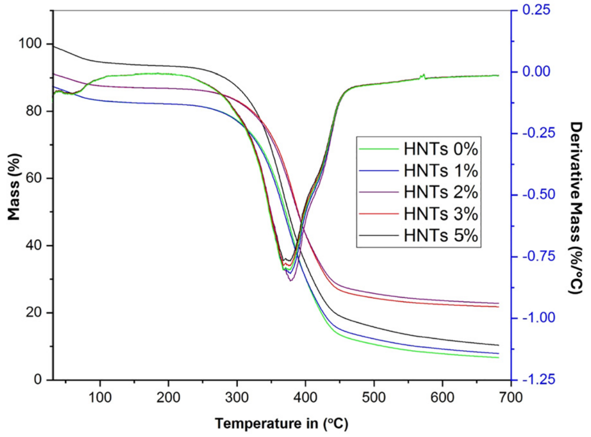

Fig. 3 TG and DTG curves of the nanocomposite materials.

variable discharge. An analysis of weight loss at various temperatures was conducted to identify the initial degradation temperature, maximum degradation temperature, and inflection point. Table 3 presents the associated values. The vaporisation of moisture in the specimen resulted in an initial weight loss, estimated at approximately 3.5%, prior to the beginning of degradation. The hydrogen bonds present in the fibers allow thermal energy to be distributed to adjacent bonds. The second stage of natural fibres breaking down and losing weight occurred when the hemicellulose and other glycosidic bonds in the fibres were heated and subsequently broken.[62,63]

The initial and final temperatures for the 2% HNT samples exceeded those of the others. The maximum weight loss occurred at the maximum degradation temperature of the specimen, and coincided with the degradation rate at the highest inflection point. In comparison to others, the 2% HNT-reinforced composite demonstrated superior inflection ranges. The composite containing 0% HNTs exhibited degradation starting at 338.08 °C and ending at 420.84 °C, with an inflection point at 388.63 °C, which is lower than that of the banana/cotton composites with HNTs. The 2% HNT nanocomposite exhibited the highest inflection point at 357.32 °C and a final degradation temperature of 452.64 °C. Cellulose decomposition begins at the maximum degradation and inflection temperatures. The residual weight of the various 2% HNT-reinforced banana/cotton hybrid composites was found to be 17.83%, which shows the complete degradation of the composite constituents. The composite containing 2% HNTs exhibited the highest thermal stability and degradation resistance. This enhancement is due to the increased interfacial adhesion between the fibres and the epoxy resin, which improves the performance of the composite materials. The TGA results provided evidence that the addition of HNTs (up to 2%) determines the thermal stabilization effect on the banana/cotton fabric, while a further addition of HNTs generates decreases in the degradation temperature.[62,63]

3.6. Chemical analysis

Fig. 4 shows the FTIR spectra of the hybrid composites with and without HNT fillers. The figure shows that the HNT fillers were successfully incorporated into the hybrid composites. The peaks present between 3400 and 3300 cm^{-1} indicate a broader spectrum depicting the strong presence of hydroxyl groups, thereby confirming the presence of cellulose and absorbed water molecules in the form of hydroxyls. C-H stretching was noted from the peaks present between 2900 and 2800 cm^{-1}, indicating the presence of lignocellulosic compounds. The peaks between 1740 and 1730 cm^{-1} correspond to the normal peak observed in the banana fibers and portray the interaction between the banana fibers and HNTs through carbonyl bonds. H–O–H bending and C═C bonds were noted between 1650 and 1640 cm^{-1}, which changed for every composite with the increase in HNT content. The bonds between 1000 and 1460 cm^{-1} indicate –CH$_2$ stretching, and Si–O–Si and C–O–C bonds portraying the incorporation of HNTs into the hybrid composites. Peaks corresponding to 950–900 cm^{-1} indicate the HNT signature characteristic band. It was also noted from the peaks that no major chemical changes occurred due to the incorporation of the HNTs, but only physical changes leading to the increase in the mechanical and thermal properties of the hybrid composites.

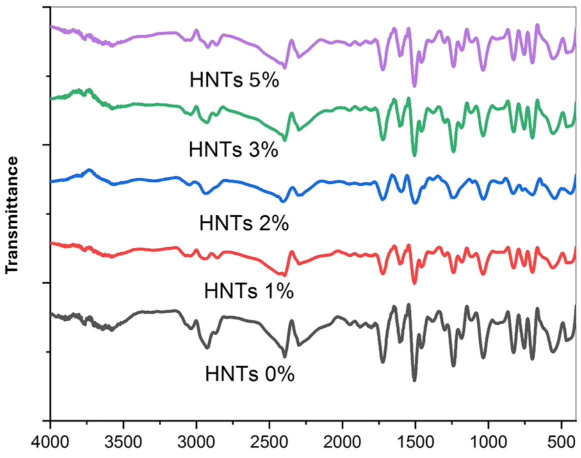

Fig. 4 FTIR spectroscopy of the nanocomposite materials.

3.7. Scanning electron microscopic analysis

Scanning electron micrographs provided evidence for the binding of resin and fabric. The SEM images clearly show the deposition of HNTs at various proportions. The images were captured at the broken end of the failed specimens under testing. A study was performed on the broken surfaces to determine how the fabric and polymer behaved in the unfilled composite and the HNT-filled composites with 1, 2, 3, and 4 weight percent of HNTs. Fig. 5 correspondingly displays the images (a, b, c, d, and e).

Examination of the images reveals that the failure of specimens is attributed to the complete deterioration of the fibre, as several instances of broken fibres are shown in all the images. This observation reveals the distinct visibility of the separation and detachment of the banana/cotton fibres from the epoxy resin. The surface of the unfilled HNT specimens exposed in Fig. 5a seems to be quite uneven, and is mostly characterised by fibre failures. This suggests that there is a deficiency of resin layers and a lack of a fibre matrix interface due to the uneven distribution of fibre aggregation inside the matrix. The failure occurs due to the initiation of debonding at the interface between the fibre and matrix, which is followed by the brittle fracture of the fibres and their pulling out, ultimately leading to the delamination of the composite. Deep pockets were observed, and were attributed to the full extraction of fibre bundles, indicating the ineffective bonding between the polymer and fibre interface, which consequently leads to distortion of the weave structure. This ultimately causes a complete separation of the contact, resulting in decreased mechanical properties.

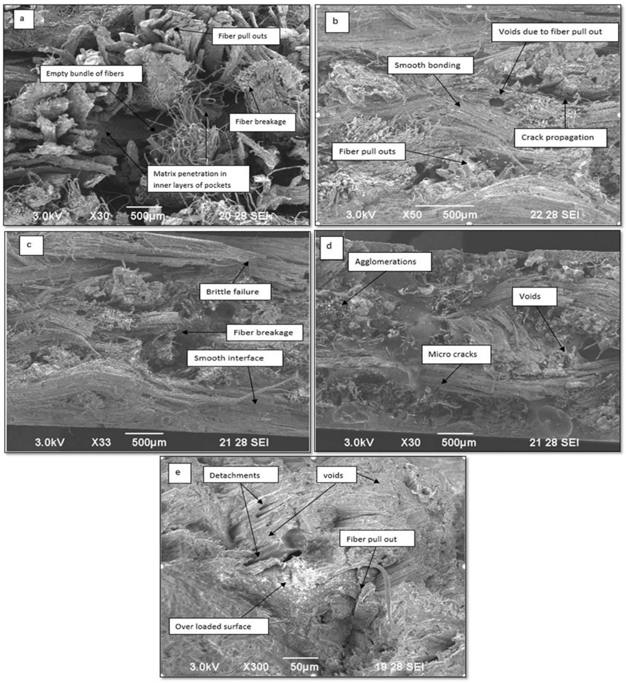

Fig. 5 SEM images of (a) 0 wt% HNT-unfilled, (b) 1 wt% HNT-filled, (c) 2 wt% HNT-filled, (d) 3 wt% HNT-filled, and (e) 4 wt% HNT-filled nanocomposites.

The SEM image in Fig. 5b of the 1 wt% HNT-filled nanocomposite reveals a relatively small, smooth area amongst the rough fibre bundles, in contrast to the surface of the unfilled composite. The interlocking of HNT-infused resin with the woven cloth creates a mild interface. The nanotubes play a crucial function in enhancing the adhesion between the resin and reinforcements. Various researchers have discovered that achieving satisfactory filler scattering with the matrix leads to higher performance as compared to pure matrix.[64,65] When fibres pull out, they leave holes in the material. These holes cause cracks to spread at stress concentration points in the specimen, but it is more structurally sound than the composite.

Fig. 5c shows the interlacing of 2 wt% HNT mixed matrix and plain fabric layers in the 4 wt% nanocomposite. The image analysis revealed a very clean surface, exhibiting an even distribution of the components. There are minimal fibre pull-outs, and the occurrence of brittle failures in the fibres is observed. The matrix and fabric interfaces exhibit excellent surface morphology, facilitating strong bonding with few flaws. The failure structure exhibits fibre damage mostly at the top, while minimising pull-outs and preventing the formation of voids by the efficient incorporation of nanoparticles. These particles enhance elasticity and hinder further damage.[66,67]

As shown in Fig. 5d, the matrix containing HNTs completely coated the surface over the fabric layers. Agglomerations are more prominent at this stage due to the poor dispersion of the HNTs. This indicates that a larger percentage (3 wt%) of HNTs is present rather than the optimal amount. The image also indicates the presence of tiny fissures, which serve as the starting point for failure by delamination. The higher the concentration of nanoparticles, the higher the viscosity of the matrix, and the lower the wettability due to the formation of agglomerations. Homogeneous distribution of HNTs in the polymer matrix increases the thermal stability (due to barrier effects on the volatile products of degradation), while the formation of HNT aggregates and/or separation phases can reduce the polymer degradation temperature.[62,68]

It is possible to see the shape of the fracture structure in Fig. 5c by adding additional HNTs to the 3 wt% nanocomposite matrix. An extensive layer of matrix completely covers the reinforcement. The interaction of overloaded HNTs with the matrix triggers the phenomenon. The figure clearly displays the occurrence of voids and micro-delamination, indicating the presence of stress concentration areas where fibers pull out. It signifies that the nanoparticles were separated from the surface of the matrix as an outcome of tension and strain caused by their poor interactions with the matrix. This diminishes the mechanical characteristics of the composite specimen.

4. Conclusions

This study emphasizes the significance of halloysite nanotubes (HNTs) reinforced in alkali-treated banana/cotton hybrid nanocomposites. The incorporation of 2 wt% HNTs significantly improved the mechanical characteristics of the composite materials, thereby increasing their suitability for structural applications. HNTs filled the interfaces, facilitated efficient load absorption and transmission. This also constrained premature fracture formation, enabling the material to withstand stress. Nonetheless, higher HNT concentrations resulted in particle agglomeration, compromising the mechanical and thermal properties of the material. The thermal stability of the 2 wt% HNT-reinforced composite exhibited enhanced resistance to any decrease, which is crucial for high-temperature applications. Morphological characteristics of the 2 wt% HNT samples exhibited satisfactory bonding between the hybrid fibres and the epoxy matrix. The improved interfacial bonding facilitated the mechanical enhancements. Nevertheless, the agglomeration of HNTs at elevated concentrations created voids and microdelamination, compromising the structural stability. This study presents a viable approach for creating high-performance, eco-friendly composites with extensive industrial applications, promoting the use of sustainable materials in the composite industry.

Author contributions

G. S. U., P. S. K., M. S. S. K. – Concept generation, Experimentation, Writing: Original Draft; A. K., K. R. - Methodology, Data curation and provided resource; M. S. S. K., M. S., L. R. K. – Writing revised draft; M. S., L. R. K. – Supervision, Data validation.

Conflicts of interest

The authors declare no personal or financial competing interests.

Data availability

No primary research results, software, or code have been included and no new data were generated or analysed as part of this review.

References

1 N. Saba, M. T. Paridah, K. Abdan and N. A. Ibrahim, Effect of Oil Palm Nano Filler on Mechanical and Morphological Properties of Kenaf Reinforced Epoxy Composites, *Constr. Build. Mater.*, 2016, **123**, 15–26.

2 H. Awais, Y. Nawab, A. Anjang, H. M. Akil and M. S. Zainol Abidin, Effect of Fabric Architecture on the Shear and Impact Properties of Natural Fibre Reinforced Composites, *Composites, Part B*, 2020, **195**, 108069.

3 S. Arivazhagan, M. Muthukumaran, T. Ganapathy, S. Dhayaneethi, D. Balaji, L. Rajeshkumar and M. Sathishkumar, Development and experimental analysis of sustainable hybrid sandwich composites from waste garlic peel and kapok bio-fillers, *Clean. Eng. Technol.*, 2026, 101174, DOI: 10.1016/j.clet.2026.101174.

4 I. D. Ibrahim, T. Jamiru, E. R. Sadiku, W. K. Kupolati and S. C. Agwuncha, Impact of Surface Modification and Nanoparticle on Sisal Fibre Reinforced Polypropylene Nanocomposites, *J. Nanotechnol.*, 2016, **2016**, 4235975.

5 F. Hanan, M. Jawaid and P. Md Tahir, Mechanical Performance of Oil Palm/KenafFibre-Reinforced Epoxy-Based Bilayer Hybrid Composites, *J. Nat. Fibres*, 2020, **17**, 155–167.

6 H. Awais, Y. Nawab, A. Amjad, A. Anjang, H. MdAkil and M. S. S. ZainolAbidin, Effect of Comingling Techniques on Mechanical Properties of Natural Fibre Reinforced Cross-Ply Thermoplastic Composites, *Composites, Part B*, 2019, **177**, 107279.

7 M. Zakriya, G. Ramakrishnan, N. Gobi, N. K. Palaniswamy and J. Srinivasan, Jute-Reinforced Non-Woven Composites as a Thermal Insulator and Sound Absorber—A Review, *J. Reinf. Plast. Compos.*, 2017, **36**, 206–213.

8 X. Xiong, S. Z. Shen, L. Hua, J. Z. Liu, X. Li, X. Wan and M. Miao, Finite Element Models of Natural Fibres and Their Composites: A Review, *J. Reinf. Plast. Compos.*, 2018, **37**, 617–635.

9 S. Sreekumar, A. Murali, A. Aravind Vasudevaru, A. Rajendran, R. Rajesh, N. Rakesh and S. R. Sreerag, Design and fabrication of pulverising unit for maximum absorptivity of raw banana fiber, in *IOP Conference Series: Materials Science and Engineering*, IOP Publishing, 2018, vol. 377, no. 1, 012039.

10 A. Amjad, H. Awais, M. Z. Ali, M. S. Z. Abidin, A. Anjang, M. S. ZainolAbidin and A. Anjang, *Effect of Alumina Nanofiller on the Mechanical Properties of 2DWoven Biotex Flax/PLA Fibre-Reinforced Nanocomposite. In Lecture Notes in Mechanical Engineering*, Springer, Singapore, 2020, pp. 383–391.

11 A. Gholampour and T. Ozbakkaloglu, A Review of Natural Fibre Composites: Properties, Modification and Processing Techniques, Characterization, Applications, *J. Mater. Sci.*, 2020, **55**, 829–892.

12 J. Yang, Y. Guo, L. Yao, Q. Ni and Y. Qiu, Effects of Kevlar Volume Fraction and Fabric Structures on the Mechanical Properties of 3D Orthogonal Woven Ramie/Kevlar Reinforced Poly (Lactic Acid) Composites, *J. Ind. Text.*, 2018, **47**, 2074–2091.

13 H. Awais, Y. Nawab, A. Amjad, A. Anjang and M. S. Z. Abidin, Mechanical Properties of Hollow Glass Microspheres Filled Jute Woven Comingled Composites, *Key Eng. Mater.*, 2020, **858**, 41–46.

14 M. S. S. Godara, Effect of Chemical Modification of Fibre Surface on Natural Fibre Composites: A Review, *Mater. Today: Proc.*, 2019, **18**, 3428–3434.

15 A. K. Bledzki, A. A. Mamun and V. S. Gutowski, The Effects of Acetylation on Properties of Flax Fibre and Its Polypropylene Composites, *eXPRESS Polym. Lett.*, 2008, **2**, 413–422.

16 K. Achuthan, S. Muthupalani and V. K. Kolil, A novel banana fiber pad for menstrual hygiene in India: a feasibility and acceptability study, *BMC Women's Health*, 2021, **21**, 129.

17 R. Vinayagamoorthy, Influence of Fibre Surface Modifications on the Mechanical Behavior of VetiveriaZizanioides Reinforced Polymer Composites, *J. Nat. Fibres*, 2019, **16**, 163–174.

18 J. Khan and M. Mariatti, The Influence of Substrate Functionalization for Enhancing the Interfacial Bonding between Graphene Oxide and Nonwoven Polyester, *Fibres Polym.*, 2021, 1–11.

19 R. De Araujo Alves Lima, D. Kawasaki Cavalcanti, J. de Souza e Silva Neto, H. Meneses da Costa and M. D. Banea, Effect of Surface Treatments on Interfacial Properties of Natural Intralaminar Hybrid Composites, *Polym. Compos.*, 2020, **41**, 314–325.

20 A. L. Pereira, M. D. Banea, J. S. S. Neto and D. K. K. Cavalcanti, Mechanical and Thermal Characterization of Natural Intralaminar Hybrid Composites Based on Sisal, *Polymers*, 2020, **12**, 866.

21 H. Abdellaoui, M. Raji, H. Essabir, R. Bouhfid and A. E. K. Qaiss, Mechanical Behavior of Carbon/Natural Fibre-Based Hybrid Composites, in *Mechanical and Physical Testing of Biocomposites, Fibre-Reinforced Composites and Hybrid Composites*, Elsevier, Amsterdam, The Netherlands, 2018, pp. 103–122.

22 M. J. Mochane, T. C. Mokhena, T. H. Mokhothu, A. Mtibe, E. R. Sadiku, S. S. Ray, I. D. Ibrahim and O. O. Daramola, Recent Progress on Natural Fibre Hybrid Composites for Advanced Applications: A Review, *eXPRESS Polym. Lett.*, 2019, **13**, 159–198.

23 S. Stankovich, D. A. Dikin, G. H. B. B. Dommett, K. M. Kohlhaas, E. J. Zimney, E. A. Stach, R. D. Piner, S. B. T. Nguyen and R. S. Ruoff, Graphene-Based Composite Materials, *Nature*, 2006, **442**, 282–286.

24 S. J. Eichhorn, A. Dufresne, M. Aranguren, N. E. Marcovich, J. R. Capadona, S. J. Rowan, C. Weder, W. Thielemans, M. Roman and S. Renneckar, *et al.*, Review: Current International Research into Cellulose Nanofibres and Nanocomposites, *J. Mater. Sci.*, 2010, **45**, 1–33.

25 K. M. F. Hasan, P. G. Horváth and T. Alpár, Potential Natural Fibre Polymeric Nanobiocomposites: A Review, *Polymers*, 2020, **12**, 1072.

26 H. Awais, Y. Nawab, A. Amjad, A. Anjang and M. S. S. ZainolAbidin, Fabrication and Characterization of Lightweight Engineered Polypropylene Composites Using Silica Particles and Flax Woven Comingled Structure, *Lecture Notes in Mechanical Engineering*, Springer, Berlin/Heidelberg, Germany, 2020, pp. 403–410.

27 J. Khan, S. A. Momin and M. Mariatti, *A Review on Advanced Carbon-Based Thermal Interface Materials for Electronic Devices*, Elsevier, Amsterdam, The Netherlands, 2020, vol. 168, pp. 65–112.

28 M. Bhattacharya, Polymer Nanocomposites-A Comparison between Carbon Nanotubes, Graphene, and Clay as Nanofillers, *Materials*, 2016, **9**, 262.

29 D. M. Marquis, É. Guillaume, C. Chivas-Joly, M. M. Damien, G. Eric and C.-J. Carine, *Properties of Nanofillers in Polymer*, Intech Open, London, UK, 2015, vol. 2, p. 64.

30 N. Saba, P. M. Tahir and M. Jawaid, A Review on Potentiality of Nano Filler/Natural Fibre Filled Polymer Hybrid Composites, *Polymers*, 2014, **6**, 2247–2273.

31 M. Manjunath, N. M. Renukappa and B. Suresha, Influence of Micro and Nanofillers on Mechanical Properties of Pultruded Unidirectional Glass Fibre Reinforced Epoxy Composite Systems, *J. Compos. Mater.*, 2016, **50**, 1109–1121.

32 M. Foruzanmehr, P. Y. Vuillaume, S. Elkoun and M. Robert, Physical and Mechanical Properties of PLA Composites Reinforced by TiO2 Grafted Flax Fibres, *Mater. Des.*, 2016, **106**, 295–304.

33 A. Samariha, A. H. Hemmasi, I. Ghasemi, B. Bazyar and M. Nemati, Effect of Nanoclay Contents on Properties, of Bagasse Flour/Reprocessed High Density Polyethylene/Nanoclay Composites, *MaderasCienc. Tecnol.*, 2015, **17**, 637–646.

34 Y. Li, C. Chen, J. Xu, Z. Zhang, B. Yuan and X. Huang, Improved Mechanical Properties of Carbon Nanotubes-Coated Flax Fibre Reinforced Composites, *J. Mater. Sci.*, 2015, **50**, 1117–1128.

35 P. K. Kushwaha, C. N. Pandey and R. Kumar, Study on the Effect of Carbon Nanotubes on Plastic Composite Reinforced with Natural Fibre, *J. Indian Acad. Wood Sci.*, 2014, **11**, 82–86.

36 M. Chaharmahali, Y. Hamzeh, G. Ebrahimi, A. Ashori and I. Ghasemi, Effects of Nano-Graphene on the Physico-Mechanical Properties of Bagasse/Polypropylene Composites, *Polym. Bull.*, 2014, **71**, 337–349.

37 S. B. Hosseini, S. Hedjazi, L. Jamalirad and A. Sukhtesaraie, Effect of Nano-SiO_2 on Physical and Mechanical Properties of Fibre Reinforced Composites (FRCs), *J. Indian Acad. Wood Sci.*, 2014, **11**, 116–121.

38 A. Gowthami, K. Ramanaiah, A. V. Ratna Prasad, K. Hema Chandra Reddy, K. Mohana Rao and G. Sridhar Babu, Effect of Silica on Thermal and Mechanical Properties of Sisal Fibre Reinforced Polyester Composites, *J. Mater. Environ. Sci.*, 2013, **4**, 199–204.

39 S. O. Han, M. Karevan, M. A. Bhuiyan, J. H. Park, K. Kalaitzidou, M. A. Bhuiyan, M. Karevan, S. O. Han and J. H. Park, Effect of Exfoliated Graphite Nanoplatelets on the Mechanical and Viscoelastic Properties of Poly(Lactic Acid) Biocomposites Reinforced with Kenaf Fibres, *J. Mater. Sci.*, 2012, **47**, 3535–3543.

40 T. D. Hapuarachchi and T. Peijs, Multiwalled Carbon Nanotubes and SepioliteNanoclays as Flame Retardants for Polylactide and Its Natural Fibre Reinforced Composites, *Composites, Part A*, 2010, **41**, 954–963.

41 S. P. Babu, Y. KK, V. MG, K. GK, D. M. Goudar, R. V. Kurahatti and S. K. Bhat, Enhanced mechanical, thermal, and wear performance of halloysite nanotube infused carbon fiber epoxy composites, *Sci. Rep.*, 2025, **15**(1), 1–25.

42 C. I. Idumah, A. Hassan, J. Ogbu, J. U. Ndem and I. C. Nwuzor, Recently emerging advancements in halloysite nanotubes polymer nanocomposites, *Compos. Interfaces*, 2019, **26**(9), 751–824.

43 N. Danyliuk, J. Tomaszewska and T. Tatarchuk, Halloysite nanotubes and halloysite-based composites for environmental and biomedical applications, *J. Mol. Liq.*, 2020, **309**, 113077.

44 M. Ertas, E. Altuntas and A. Donmez Cavdar, Effects of halloysite nanotube on the performance of natural fiber filled poly (lactic acid) composites, *Polym. Compos.*, 2019, **40**(11), 4238–4247.

45 Y. Chen, L. M. Geever, J. A. Killion, J. G. Lyons, C. L. Higginbotham and D. M. Devine, Halloysite nanotube reinforced polylactic acid composite, *Polym. Compos.*, 2017, **38**(10), 2166–2173.

46 H. S. Aljibori, A. Al-Amiery and W. N. R. W. Isahak, Unveiling the potential of halloysite nanotubes: insights into their synthesis, properties, and applications in nanocomposites, *Starch-Stärke*, 2025, **77**(3), 2400080.

47 Y. Wu, Y. Zhang, J. Ju, H. Yan, X. Huang and Y. Tan, Advances in halloysite nanotubes–polysaccharide nanocomposite preparation and applications, *Polymers*, 2019, **11**(6), 987.

48 S. Kamarian, R. Barbaz-Isfahani, T. M. N. Tran and J. I. Song, Optimal flammability and thermal buckling resistance of eco-friendly abaca fiber/polypropylene/egg shell powder/halloysite nanotubes composites, *Adv Nano Res.*, 2024, **16**, 127–140.

49 Z. Jiang, S. Sun, J. Liu and X. Sun, Recent advances of halloysite nanotubes in biomedical applications, *Small*, 2024, **20**(2), 2306169.

50 T. Islam, M. H. Chaion, M. A. Jalil, A. S. Rafi, F. Mushtari, A. K. Dhar and S. Hossain, Advancements and challenges in natural fiber-reinforced hybrid composites: a comprehensive review, *SPE Polymers*, 2024, **5**(4), 481–506.

51 A. Garg, S. Basu, R. L. Mahajan and R. Mehta, Enhancement in mechanical properties of GFRP-coal-derived graphene oxide composites by addition of multiwalled carbon nanotubes and halloysite nanotubes: A comparative study, *Polym. Compos.*, 2024, **45**(14), 13164–13179.

52 X. Jin, J. Li, R. Zhang, Z. Jiang and D. Qin, Fabrication of high-performance bamboo–plastic composites reinforced by natural halloysite nanotubes, *Molecules*, 2020, **25**(9), 2259.

53 M. Azami, A. K. Maurya and A. Ameli, Recent Advances in the Processing of Halloysite Nanotubes–Polymer Nanocomposites, *Hybrid Composite Materials: Experimental and Theoretical Analysis*, 2024, pp. 293–313.

54 A. Jenifer, N. Rasana and K. Jayanarayanan, Synergistic effect of the inclusion of glass fibers and halloysite nanotubes on the static and dynamic mechanical, thermal and flame-retardant properties of polypropylene, *Mater. Res. Express*, 2018, **5**(6), 065308.

55 S. P. Lonkar, S. Therias, N. Caperaa, F. Leroux and J. L. Gardette, 'Photo oxidation of polypropylene/layered doubled hydroxide nanocomposites: influence of intra lamellar cations', *Eur. Polym. J.*, 2010, **46**(7), 1456--1464ISSN: 0014-3057.

56 T. D. Fornes, P. J. Yoon and D. R. Paul, Polymer matrix degradation and colour formation in melt processed nylon 6/clay nanocomposites, *Polymer*, 2003, **44**(24), 7545–7556ISSN: 0032-3861.

57 R. S. Shah and D. R. Paul, 'Organoclay degradation in melt processed polyethylene nanocomposites', *Polymer*, 2006, **47**(11), 4075–4084ISSN: 0032-3861.

58 A. Yasmin, J. J. Luo, J. L. Abot and I. M. Daniel, 'Mechanical and thermal behaviour of clay/epoxy nano composites', *Compos. Sci. Technol.*, 2006, **66**(14), 2415–2422ISSN: 0266-3538.

59 S. Siriwardena, H. Ismail and S. Ishiaku, 'A comparison of the mechanical properties and water absorption behaviour of white rice husk ash and silica filled polypropylene composites', *J. Reinf. Plast. Compos.*, 2003, **22**, 1645–1666ISSN: 0731-6844.

60 J. Chandradass and D.-S. Bae, Preparation and properties of barium titanatenano powder/epoxy composites, *Mater. Manuf. Processes*, 2008, **23**(2), 116–122, ISSN: 1042-6914.

61 P. Mareri, S. Bastide, N. Binda and A. Crespy, Mechanical behaviour of polypropylene composites containing fine mineral filler: Effect of filler surface treatment', *Compos. Sci. Technol.*, 1998, **58**(5), 747–752ISSN: 0266-3538.

62 G. Cavallaro, G. Lazzara and S. Milioto, Nanocomposites based on halloysite nanotubes and sulphated galactan from red seaweed Gloiopeltis: Properties and delivery capacity of sodium diclofenac, *Int. J. Biol. Macromol.*, 2023, **234**, 123645.

63 M. R. Caruso, G. D'Agostino, G. Cavallaro, O. Gómez-Laserna, M. Maguregui and G. Lazzara, Chitosan/halloysite clay mixture for preservation of waterlogged archaeological woods, *Int. J. Biol. Macromol.*, 2025, 147126.

64 O. Kamigaito, 'What can be improved by nanometer composites,', *J. Jpn. Soc. Powder Powder Metall.*, 1991, **38**, 315–321ISSN: 0532-8799.

65 J. E. Mark, C. Y. Jiang and M. Y. Tang, 'Simultaneous curing and filling of elastomers', *Macromolecules*, 1984, **17**(12), 2613–2616ISSN: 0024-9297.

66 J. Y. Wen and G. L. Wilkes, 'Organic/inorganic hybrid network materials by the sol-gel approach', *Chem. Mater.*, 1996, **8**(8), 1667–1681ISSN: 0897-4756.

67 A. J. Heeger, 'Semiconducting polymers: The third generation', *Chem. Soc. Rev.*, 2010, **39**(7), 2354–2371ISSN: 0306-0012.

68 Y. Xu and S. V. Hoa, 'Mechanical properties of carbon fibre reinforced epoxy/clay nanocomposites', *Compos. Sci. Technol.*, 2008, **68**(3–4), 854–861ISSN: 0266-3538.